Molecular Vision 2017; 23:334-345 <http://www.molvis.org/molvis/v23/334>
Received 8 June 2016 | Accepted 14 June 2017 | Published 16 June 2017

Meclofenamic acid improves the signal to noise ratio for visual responses produced by ectopic expression of human rod opsin

Cyril G. Eleftheriou, Jasmina Cehajic-Kapetanovic, Franck P. Martial, Nina Milosavljevic, Robert A. Bedford, Robert J. Lucas

Faculty of Biology Medicine and Health, University of Manchester, Manchester Academic Health Sciences Centre, Manchester, UK

Purpose: Retinal dystrophy through outer photoreceptor cell death affects 1 in 2,500 people worldwide with severe impairment of vision in advanced stages of the disease. Optogenetic strategies to restore visual function to animal models of retinal degeneration by introducing photopigments to neurons spared degeneration in the inner retina have been explored, with variable degrees of success. It has recently been shown that the non-steroidal anti-inflammatory and non-selective gap-junction blocker meclofenamic acid (MFA) can enhance the visual responses produced by an optogenetic actuator (channelrhodopsin) expressed in retinal ganglion cells (RGCs) in the degenerate retina. Here, we set out to determine whether MFA could also enhance photoreception by another optogenetic strategy in which ectopic human rod opsin is expressed in ON bipolar cells.

Methods: We used in vitro multielectrode array (MEA) recordings to characterize the light responses of RGCs in the *rd*[1] mouse model of advanced retinal degeneration following intravitreal injection of an adenoassociated virus (AAV2) driving the expression of human rod opsin under a minimal grm6 promoter active in ON bipolar cells.

Results: We found treated retinas were light responsive over five decades of irradiance (from 10^{11} to 10^{15} photons/cm^2/s) with individual RGCs covering up to four decades. Application of MFA reduced the spontaneous firing rate of the visually responsive neurons under light- and dark-adapted conditions. The change in the firing rate produced by the 2 s light pulses was increased across all intensities following MFA treatment, and there was a concomitant increase in the signal to noise ratio for the visual response. Restored light responses were abolished by agents inhibiting glutamatergic or gamma-aminobutyric acid (GABA)ergic signaling in the MFA-treated preparation.

Conclusions: These results confirm the potential of MFA to inhibit spontaneous activity and enhance the signal to noise ratio of visual responses in optogenetic therapies to restore sight.

Photoreceptor apoptosis is a common cause of blindness [1,2]. In this condition, elements of the inner retina survive in a state of deafferentation. One therapeutic approach for this condition is to attempt to restore visually evoked patterns of electrophysiological activity to the surviving neurons in the hope that they will propagate to the brain. Implanted electronic devices that directly excite surviving neurons of the inner retina according to the pattern of light exposure restore some sight in such patients [3,4]. Nanophotovoltaic strategies, such as optogenetics [5-7], azobenzene photoswitches [8-11], or even quantum-dot conjugated carbon-nanotubes [12], have been proposed as alternative approaches to rendering the surviving inner retina light sensitive without having to implant complex electronic devices in such a delicate portion of the central nervous system (CNS).

Although the inner retina appears to be relatively well preserved in the dystrophic retina of humans and animal models, deafferentation induces remodeling of retinal circuits [13-15] and hyperactivity in retinal ganglion cells (RGCs) [16-18] characterized by bursts of action potentials recurring at regular (about 10 Hz) intervals. These oscillations traveling across the RGC syncytium at speeds of 3–8 mm/s [19,20] are driven by fluctuations in the voltage membrane of one type of amacrine cells (ACs), AII (AII ACs), electrically coupled to ON cone bipolar cells [21,22]. Application of meclofenamic acid (MFA), a potent gap junction blocker, can decouple AII ACs from ON cone bipolar cells leading to the removal of the hyperactive spiking of RGCs [23,24]. Using MFA to remove this pathological hyperactivity in partially rehabilitated retinas has been reported to improve the bioelectric signal generated by one optogenetic actuator (channelrhodopsin) when expressed in RGCs [25,26]. Here, we set out to test the generalizability of that finding to ask whether it can be extended to a therapeutic intervention using a photopigment (human rod opsin) with a quite different mode of action and targeted for expression elsewhere in the retinal circuitry (ON bipolar cells) [27].

Correspondence to: Cyril Eleftheriou; Faculty of Life Sciences, University of Manchester, M13 9PT Manchester, UK; Phone: +44161 275 5050; FAX: ??; email: cyril.eleftheriou@manchester.ac.uk

METHODS

Viral injections: Adult C3H mice were used in this study. All animal experiments and care were conducted in accordance with the UK Animals (Scientific Procedures) Act of 1986 (UK) and approved by the University of Manchester ethical review committee. Animals were kept in a 12 h:12 h light-dark cycle at a temperature of 22 °C with food and water available ad libitum. Experiments were undertaken in mice between 8 and 12 weeks after intravitreal injection of adenoassociated virus (AAV) vector administered in mice anaesthetized with ketamine (80 mg/kg, Narketan-10, 100 mg/ml, Ventoquinol, Buckingham, UK) and xylazine (8 mg/kg, Rompun 2% w/v, Bayer, Kansas City, KS) between 8 and 10 weeks of age. Each eye was injected with 3 µl of virus (10^{13} genomic counts) containing a rod opsin (AAV2-ITR-grm6-RHO-polyA-WPRE-ITR) expression construct, in combination with 0.5 ml of glycosidic enzyme solution containing 0.125 units each of hyaluronan lyase and heparinase III (E.C. 4.2.2.1 and E.C. 4.2.2.8; Sigma, Irvine, UK).

Electrophysiological recordings: The mice were euthanized by cervical dislocation and immediately enucleated. Retinal dissections were performed under fluorescent white light in carboxygenated (95% O_2/5% CO_2) artificial cerebrospinal fluid (aCSF, concentration in mM: 118 NaCl, 25 $NaHCO_3$, 1 NaH_2PO_4, 3 KCl, 1 $MgCl_2$, 2 $CaCl_2$, 10 $C_6H_{12}O_6$, 0.5 L-glutamine; Sigma-Aldrich).

While the eyes were maintained with a pair of thick forceps, the edge of the cornea was pierced with a hypodermic needle (23 gauge, Microlance, Becton Dickinson, Franklin Lakes, NJ). Then, the cornea was sheared along the ora serrata with vannas scissors (WPI, Worcester, MA), and the lens was gently removed from the eye cup. In these animals, the retina was often stuck to the lens (possibly due to digestion of the internal limiting membrane (ILM) by the enzymes injected with the virus or inflammation secondary to the intravitreal injection). Therefore, the retina had to be isolated from the lens with two pairs of Dumont #5 forceps (WPI) by delicately pulling at the ora serrata.

The retina was incised multiple times at the edges to maximize planarization and then mounted ganglion cell layer (GCL) down on a transparent 256 channel Multi Electrode Array (MEA; 256MEA200/30iR-ITO; Multi Channel Systems GmbH, Reutlingen, Germany). A Cyclopore membrane (5 µm pores; Whatman Plc, Little Chalfont, UK) held the retina in place while weighted down by two stainless steel anchors (about 0.75 g each) bearing a framework of parallel polyimide-coated fused silica capillaries (TSP320450, Polymicro Technologies, MOLEX LLC, Lisle IL).

Electrophysiological signals were sampled at 25 kHz using MC_Rack software through a USB-MEA256 amplifier (Multi Channel Systems). To record the extracellular action potentials, the electrophysiological signals were filtered (200 Hz high pass, Butterworth second order) and thresholded (4 standard deviations below the noise level) online. Raw, un-thresholded, un-filtered data files of 1 min durations were collected between the application of each pharmacological agent to monitor the impact on the local field potentials. The explanted retina was perfused with carboxygenated aCSF at 2.2 ml/min supplemented with 4 µM 9-cis-retinal (Sigma Aldrich) using a peristaltic pump (120 U, Watson Marlow, Falmouth, UK) and maintained at 32 °C using a TC01 controller (Multi Channel Systems) that regulated the temperature of the copper plate below the MEA.

Pharmacology: Blocking of various synapses was achieved by bath applying various pharmacological substances dissolved in aCSF, which superfused the explanted retina as described. Gap junctions were blocked with 50 µM MFA (Sigma Aldrich) that was applied for 30 min before the data were recorded. Glutamatergic signaling was blocked using a combination of three compounds: 100 µM 6,7-dinitroquinoxaline-2,3-dione (DNQX; Tocris Bioscience, Bristol, UK) was used to block the α-amino-3-hydroxy-5-methyl-4-isoxazolepropionic acid (AMPA)-type glutamatergic synapses, 100 µM DL-AP5 (Tocris Bioscience) was used to block the N-methyl-D-aspartate (NMDA) glutamatergic synapses, and 150 µM DL-AP4 (Tocris Bioscience) was used to block the metabotropic (mGluR6) synapses. As an mGluR6 agonist, DL-AP4 did not allow the investigation of synapses downstream of the transfected ON bipolar cells. Gamma-aminobutyric acid (GABA)a and GABAc receptors were antagonized with 20 µM picrotoxin and 50 µM 1,2,5,6-tetrahydropyridin-4-yl)methylphosphinic acid (TPMPA), respectively (Tocris Bioscience).

Light stimulation: Full-field light stimuli were delivered to the GCL from below with a violet (420 nm ƛ max) light-emitting diode (LED; M420L3, Thorlabs, Ely, UK) or a more powerful blue (470 nm ƛ max) LED (PhlatLight, Luminus Devices, Sunnyvale, CA). At full brightness, the violet LED displayed an irradiance (in photons/cm^2/s) of 3×10^{13} for rod opsin while the blue LED displayed an irradiance of 1.66×10^{15} for rod opsin. The blue LED was used only to apply the strongest stimulus. Delicate mixing of colors was regulated with 12 bit pulse width modulation in an Arduino Due (Arduino, Ivrea, Italy) controlled by custom scripts written in LabView (National Instruments, Austin, TX). Overall brightness was reduced by up to four orders of magnitudes with a circular neutral-density (ND) rotor (100FS04DV.4, Newport, Irvine

CA) controlled by a NSC200 controller system (Newport Corp.).

Response analysis: Spike files (.MCD) were merged offline in MC_DataTool (Multi Channel Systems), and the waveforms were sorted in Offline Sorter (Plexon, Dallas, TX). Spike-times were observed in NeuroExplorer (Nex, Herndon, VA) and then further analyzed in Matlab (The Mathworks, Natick, MA), using a set of custom written scripts.

Light-driven responses were classified as positive when the average spike count in the 2 s following stimulus onset was higher than the average spike count in the 2 s preceding the stimulus plus two times the standard deviation (95% confidence interval) in at least six out of seven trials. Trial bin count (TBC) figures were generated in Matlab and then imported as enhanced metafiles into CorelDraw X3 (Corel, Ottawa, Canada). Peri-stimulus time histograms (PSTHs) were generated in Matlab, imported as number matrices into Prism 6 (Graphpad, La Jolla, CA) where they were generated as graphs, and then imported as enhanced metafiles into Corel Draw.

Response onset latency was calculated from the average PSTH in 200 ms bins (unsmoothed) while response offset latency was calculated from an average PSTH in 3 ms bins and smoothed twice using a sliding window of 1,000 bins. Onset was determined when the averaged PSTH crossed the response threshold while offset was determined as the last point above the response threshold in the 18 s following stimulus extinction. The change in the firing rate (ΔFR) was calculated by subtracting μBL from μS with μBL corresponding to the average firing rate (across seven trials) in the 2 s immediately preceding the stimulus and μS corresponding to the average maximal firing rate in the 2 s immediately following the stimulus. The signal to noise ratio (SNR) was calculated with the following equation:

$$SNR = \mu S - \mu BL / \mu S + \mu BL$$

This equation deviates somewhat from other measures of SNR that divide a measure of the signal by the standard deviation of the noise. In preparations where MFA was applied, some neurons were silent resulting in a baseline of 0 spikes/s and an infinitely high SNR value. This equation caps the SNR value at 1, allowing us to perform appropriate statistical analyses.

Power spectral density (PSD) analysis was performed in Matlab on the spontaneous firing over a 2 min period using a Hanning window and 1,024 fast Fourier transform points. To detect narrow-band peak frequencies, the PSD was normalized over the surface area and subjected to an empirically established threshold of 9%.

Histology: Immunohistochemistry (IHC) was performed as described [5]. Briefly, infected eyecups were fixed in 4% paraformaldehyde (PFA) for 24 h at 4 °C, washed in 0.01 M PBS (MFCD00131855, Sigma Aldritch, Irvine, UK), cryo-protected in 30% sucrose, and horizontally sectioned (8–10 μm thickness from the ventral to the dorsal side) on a cryostat (Leica Microsystems, Wetzlar, Germany). The sections were background blocked with PBS and 0.2% Triton X-100 containing 10% donkey serum (D9663; Sigma-Aldrich) for 1 h at room temperature. Primary antibody (rabbit anti-human rhodopsin, Ab112576, 1:200 dilution; Abcam, Cambridge, UK) in blocking buffer (PBS with 0.2% Triton X-100 and 2.5% donkey serum) was applied for 2 h at room temperature. Secondary antibody (Alexa Fluor® 546 donkey anti-rabbit immunoglobulin G (H^+L) antibody, lot: 1,504,518, 1:200 dilution; Life Technologies, Warrington, UK) was applied for 2 h at room temperature. Slides were mounted with 4',6-diamidino-2-phenylindole (DAPI) containing mounting medium (Vectashield, Vector Laboratories Ltd., Peterborough, UK) to stain the cell nuclei. Retinal sections were analyzed under an Olympus BX51 upright microscope using a 20X Plan Fln objectives and captured using a CoolSNAP ES camera (Photometrics, Tucson, AZ) through MetaVue software (Molecular Devices Ltd., Wokingham, UK). Images were taken under specific band pass filter sets, and color-combined images were used for further processing using ImageJ.

RESULTS

Spontaneous variations in the spiking rate and local field potential (LFP) are typically observed in the degenerated retina [19,25]. We found such variations in the recordings of the rd1 retinas maintained in the dark. Thus, a visual inspection of the raw extracellular signal from the multielectrode array revealed marked modulations in local voltage and irregular spontaneous spike firing (see Figure 1A, top for a representative example). PSD analysis for spiking activity revealed variations over a wide range of frequencies, peaking around 4 Hz (see Figure 1B for a representative example and Figure 1C-E for population; n = 9 retinas, Wilcoxon matched-pairs signed-rank test, p = 0.0078). As previously reported, bath application of 50 μM MFA suppressed rhythmic components (see Figure 1A bottom for a representative example; Figure 1C, Wilcoxon matched-pairs signed-rank test across a population of 417 RGCs from nine retinas, $p<0.0001$) and dramatically reduced the spontaneous firing rate (Figure 1D; Wilcoxon matched-pairs signed-rank test across a population of 417 cells from nine retinas, $p<0.0001$).

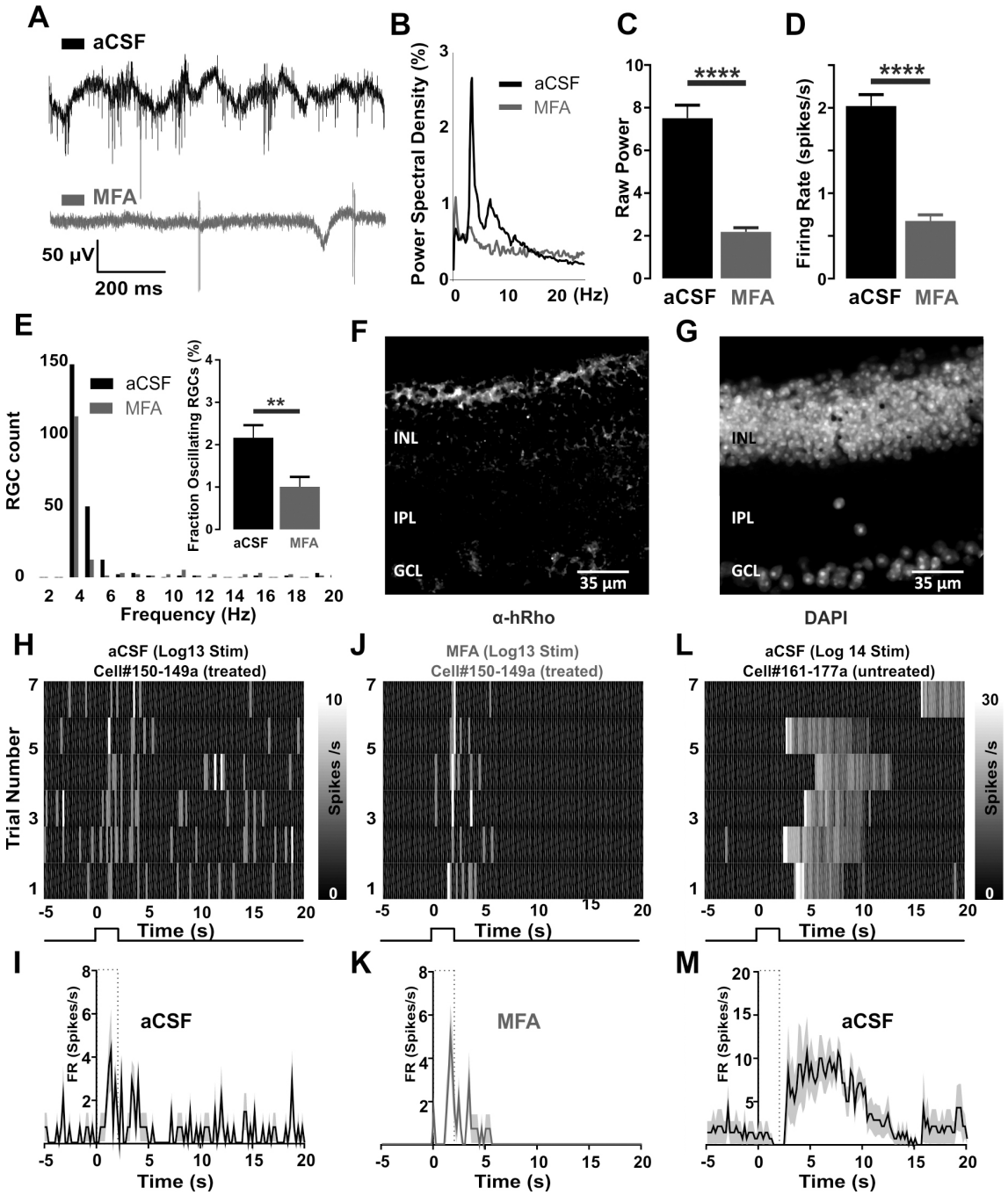

Figure 1. Impact of MFA on spontaneous and response firing. **A**: Example raw traces of extracellular activity showing the same channel under control (artificial cerebrospinal fluid [aCSF]) and meclofenamic acid (MFA) conditions. **B**: Power spectral density (PSD) of spiking in (**A**). **C**-**D**: Bar graphs representing the average (± standard error of the mean [SEM]) raw overall power (**C**) and spontaneous firing rate (**D**) of all recorded retinal ganglion cells (RGCs); n = 417 cells. **E**: Distribution of the peak frequencies of all recorded RGCs crossing a normalized power threshold of 9%. Insert: Fraction of RGCs with a maximum normalized power value exceeding 9%; n = 9 retinas. **F**-**G**: Retinal section from adult C3H rd1 mouse treated with adenoassociated virus (AAV2)-grm6-Rho and fluorescently tagged for rhodopsin (**F**) and nucleic acid (**G**). The signal from the rhodopsin antibody is present in the outer portion of the inner nuclear layer (INL), where the cell bodies of ON bipolar cells reside [32]. **H**-**K**: Example trial bin counts (TBCs; **H**, **J**) and peri-stimulus time histogram (PSTH; **J**, **K**) of cells in aCSF (**H**, **I**) and MFA (**J**, **K**) conditions responding to a 2 s stimulus (epoch indicated by dotted box and square-wave diagrams) at an irradiance of 10^{13} photons/cm^2/s from a dark background. **L**-**M**: Example TBC (**L**) and PSTH (**M**) of the melanopsin-mediated light response in the untreated retina to a stimulus of irradiance of 10^{14} photons/cm^2/s. DAPI = 4',6-diamidino-2-phenylindole; GCL = ganglion cell layer; IPL = inner plexiform layer. ** p= 0.0078, **** p<0.0001.

Viral transfection following intravitreal injection of AAV2-grm6-Rho is expected to drive expression of human rod opsin in ON bipolar cells [28-30]. Consistent with this expectation, immunohistochemical analysis of the treated retinas revealed immunoreactivity for human rhodopsin in the inner nuclear layer (Figure 1F-G), where the cell bodies of the ON bipolar cells reside [31].

Previous studies have reported that ectopic expression 200 of human rod opsin in ON bipolar cells of the rd/rd retina allows light-evoked changes in firing at the RGC level to be recorded [27,28]. We studied the effect of MFA on 18 RGCs (from the AAV2-grm6-Rho–treated retinas) showing a significant response (firing rate during stimulus >2 standard deviations over the mean baseline on at least six of the seven stimulus presentations) to a 2 s 10^{13} photons/cm^2/s full-field stimulus under perfusion with aCSF (shown for a representative single unit in Figure 1H-I). Under the influence of MFA, the light responses appeared more obvious, with bursts of spikes following the stimulus presentation in the neurons with low baseline activity (a representative unit is shown in Figure 1J-K). This effect was apparent across the population of light-responsive units with the mean peak change in the firing rate statistically significantly larger in the MFA-treated retinas (Figure 2G; n = 18 RGCs; Sidak's multiple comparisons test, p = 0.0079). This effect translated into a substantial increase in the SNR (see the Methods section) of the visual response following the application of MFA (Figure 2H; n = 18 RGCs, Sidak's multiple comparisons test, p<0.0001).

To exclude the possibility that MFA simply increases the likelihood of observing endogenous, melanopsin-driven visual responses, we applied the same protocol to age matched control retinas. MFA effectively silenced firing in these preparations leaving mean ± SEM spontaneous activity at 0.67 spikes/s. The 2 s 10^{13} photons/cm^2/s full-field stimulus had no noticeable effect on firing. Thus, we did not find any units that met the response criterion (firing rate during stimulus >2 standard deviations over mean baseline on at least six of the seven trials). Two units responded when we increased the stimulus intensity to 10^{14} photons/cm^2/s, with extremely slow on and offset kinetics typical of melanopsin-driven responses and quite different from the typical response of treated retinas (a representative unit is shown in Figure 1L-M).

To explore the impact of MFA on responses over a wide range of light levels, we adjusted the intensity of the 2 s flash over six decades from 3×10^{10} to 1.66×10^{15} photons/cm^2/s. We found examples of units responding over at least four decades of light intensity under the aCSF and MFA conditions (Figure 2A-D). There were no convincing responses at the lowest light intensity. At higher intensities, the response profile appeared to vary between units and across stimulus intensities. In all cases, there was an increase in firing associated with the stimulus, but this could be preceded by a suppression of firing (e.g., see Figure 2A,C, Cell #147_01b at higher intensities). The response latency for the increase in firing also varied although, as previously reported, in some instances it was <500 ms (Figure 2E). MFA increased the response firing rate and the SNR across the intensity range (Figure 2G-H; n = 18 RGCs, two-way ANOVA with post-hoc Sidak's multiple comparisons test; four stars indicate p<0.0001; for ΔFR, p values were 0.0462, 0.0041, and 0.0079 for irradiances at log 12, 13, and 14 photons/cm^2/s) without statistically significantly affecting the onset latency (Figure 2F; Mann–Whitney test across 15 RGCs, p = 0.2842).

Any optogenetic therapy must aim to function under light-adapted conditions if it is to support dynamic vision. We have previously reported that rod opsin can provide such activity, and that was the case in the preparations studied here. Thus, of 18 visually responsive units, we found that nine had a statistically significant modulation in firing when presented with a 2 s 50X or 100X intensity step against a steady 10^{12} photons/cm^2/s background (representative units shown in Figure 3A,B). Therefore, we wished to determine whether the stabilizing effects of MFA were also active under light-adapted conditions. We found that MFA reduced the spontaneous firing rate and minimized the periodic activity in the light-responsive units across two background light intensities (Figure 2C,D; n = 9 RGCs, two-way ANOVA with Bonferroni's multiple comparisons test, p<0.0001, vertical asterisks). Although the firing rate was not statistically significantly affected by background light (Friedman tests; p = 0.3476 and p = 0.3761 for MFA and aCSF, respectively), oscillatory power was statistically significantly reduced with background irradiance under MFA (Figure 2D; n = 9 RGCs, Friedman test with Dunn's multiple comparisons test; p = 0.0006 and p<0.0001 for log 10 and 11 photons/cm^2/s, respectively).

In the absence of MFA, rod opsin expressed in ON bipolar cells drives mainly excitatory responses in ganglion cells via glutamatergic and GABAergic signaling [27,28]. We finally checked that this fundamental circuit was still responsible for visual responses in the presence of MFA. We found that responses to 2 s stimuli under MFA were abolished by picrotoxin and TPMPA, antagonists of the GABAa and GABAc receptors, respectively (Figure 4B). A cocktail of inhibitors of glutamatergic signaling (ACET, L-AP4, and DNQX) had each component applied sequentially and in different orders. The final cocktail, containing all three blockers, abolished all responses to the 2 s stimulus (Figure 4A). Responses were

also lost when DNQX was applied earlier in the sequence but sometimes survived L-AP4 and ACET alone or in combination (Data not shown as those occurrences were rare and not systematically reproduced across experiments). Together, these data are consistent with the hypothesis that the visual signal produced by ectopic rod opsin reaches ganglion cells via ionotropic glutamate and GABAergic synapses. One possible route consistent with these observations and known retinal circuitry is shown in Figure 4C.

DISCUSSION

Here, we demonstrated the use of MFA to reduce aberrant pathophysiological spiking in the RGC layer of degenerated retinas, resulting in an increased SNR for and a ΔFR in the light responses originating with rod opsin virally expressed in ON bipolar cells. Barrett et al. [25] found a significant increase in the SNR and the number of responses with the bath application of 40 μM MFA in the degenerated retinas of mice genetically engineered to express channelrhodopsin in RGCs (mouse line) in response to light stimuli 25.5 μW/

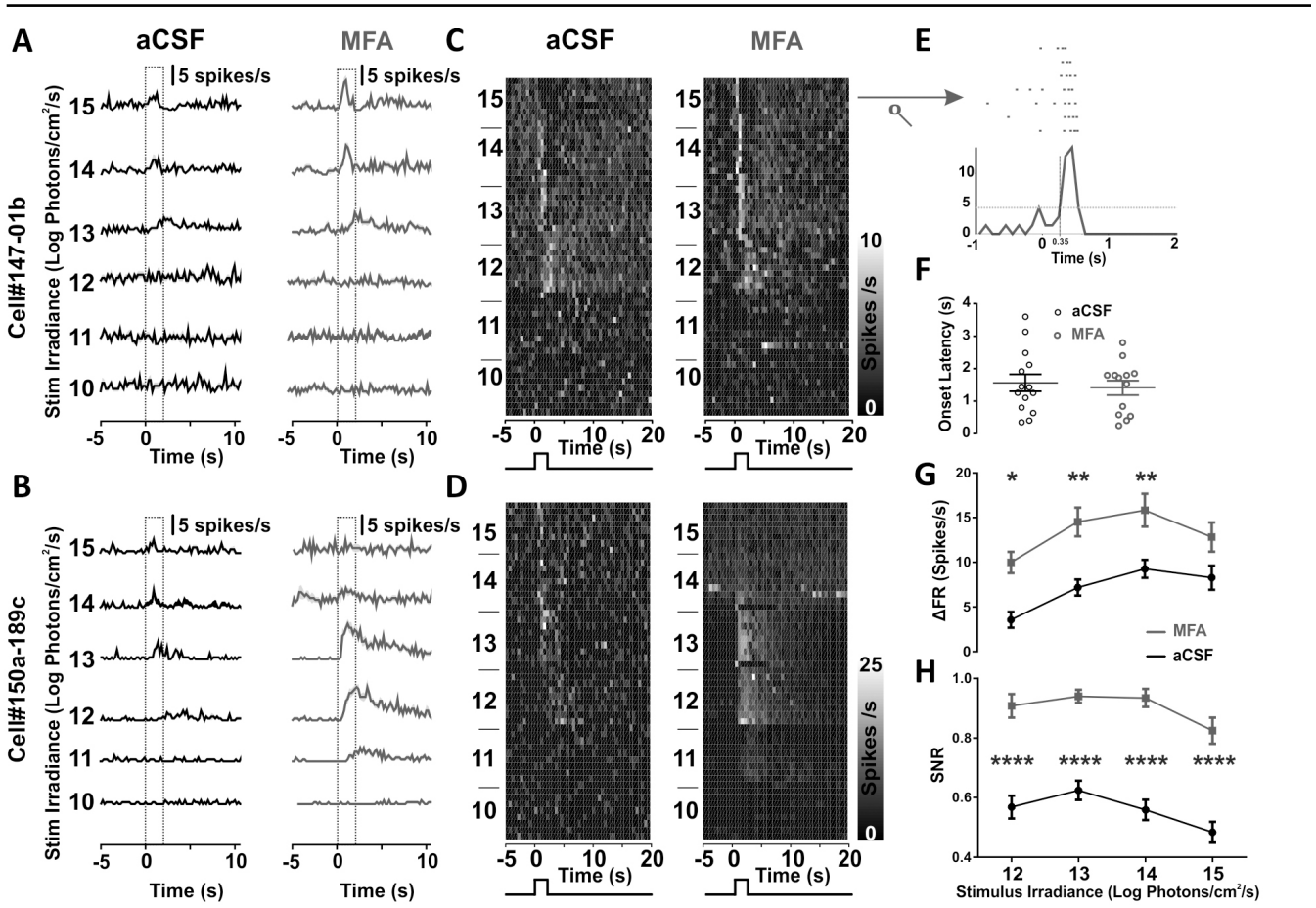

Figure 2. Irradiance sensitivity of retinal ganglion cells from Rh-grm6 transfected retinas. **A**-**B**: Average peri-stimulus time histograms (PSTH; mean ± standard error of the mean [SEM]) across the trials for two example single units (**A** and **B**) as a function of stimulus irradiance for artificial cerebrospinal fluid (aCSF; left) and meclofenamic acid (MFA; right) conditions. Dotted box indicates the stimulus epoch. **C**-**D**: Example trial bin counts (TBCs) of cells in (**C** and **D** respective for **A** and **B**) for control (left) and MFA (right) conditions. Square-wave diagram indicates stimulus epoch. Trials are stacked in decreasing order of stimulus irradiance from top to bottom. **E**: Perievent raster of response to highest intensity for cell in (**A**) showing the fine timing of the response onset. **F**: Population data for all responding cells displaying onset latency at stimulus irradiance giving the largest response for each cell; n = 15 retinal ganglion cells (RGCs). **G**-**H**: Population data for all responding cells displaying the mean (± SEM) of the change in the firing rate (ΔFR; **G**) and the signal to noise ratio (SNR; **H**) across all trials as a function of the stimulus irradiance. Asterisks indicate a statistically significant difference between aCSF and MFA at that condition; n = 18 RGCs. * p=0.0462(log12), ** p= 0.0041 (log13), ** p= 0.0079 (log14), **** p<0.0001.

mm^2 in irradiance. As previously reported [27,28], we found ectopically expressed rhodopsin to be several orders of magnitude more sensitive than channelrhodopsin. Thus, our dimmest suprathreshold stimulus had an irradiance of 5.1 10^{-4} μW/mm^2 (380–447 nm, ƛ max 406 nm, 3×10^{12} photons/cm^2/s) making it almost 50,000 times dimmer than used by Barrett et al. [25] to record visual responses evoked by channelrhodopsin. Although both studies reported an improvement in response discrimination in vitro, these findings do not necessarily translate to advanced visual discrimination in a treated animal, extending the scope for further in vivo and behavioral studies.

The change in the firing rate driven by ectopic rod opsin observed in the present study is modest compared with that produced by residual cones in young *rd*[1] retinas (up to 200 spikes/s at P15 [16]) or direct electrical stimulation of RGCs in *rd*[1] retinas (up to 60 spikes/s [32]). This result further highlights the need to optimize ON bipolar cell transfection (more transfected bipolar cells converging on an RGC is expected to give a higher response signal), as well as the light transduction mechanisms of ectopically expressed photopigments. As the general conclusions of the present analyses are based on precise, single RGC responses, the spike sorting criteria were stringent, excluding many multiunit waveforms. Therefore, these criteria affected the total firing rate, encompassing the spontaneous and response firing rates.

Although the responses under the control conditions were readily detectable, those under the MFA conditions had a consistently higher SNR and ΔFR. The higher SNR and increase in detectability are most likely due to the absence of aberrant spontaneous activity following decoupling of intrinsically oscillating AII ACs from the ON cone bipolar cells [21,22]. With the grm6 promoter restricting ectopic rod opsin expression to ON bipolar cells [27,28], under the control

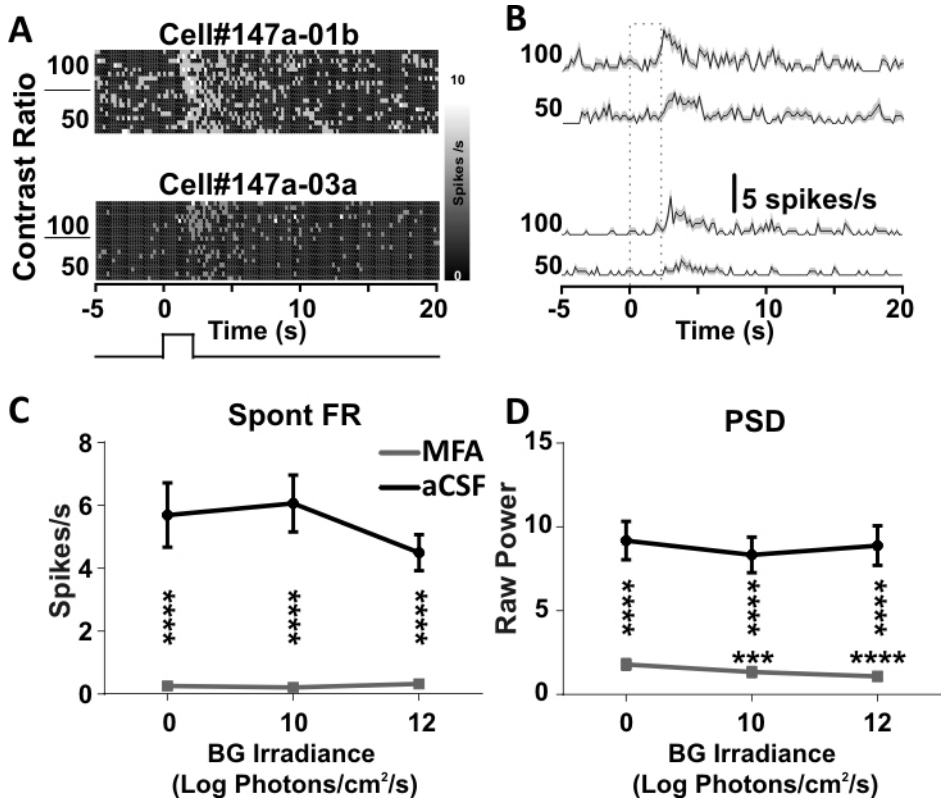

Figure 3. Activity under light-adapted conditions. **A**: Responses (trial bin counts [TBCs]) of two example retinal ganglion cells (RGCs) to 50- and 100-fold increases in irradiance (figures to left, ten trials per condition; square-wave diagram below indicates the stimulus epoch). **B**: Peri-stimulus time histogram (PSTH) showing the mean (± standard error of the mean [SEM]) firing rate across each step condition (the dotted box indicates the stimulus epoch) for cells in **A**. **C**: Average (± SEM) spontaneous firing rate (spikes/s) of the visually responsive cells under dark-adapted conditions and at two background light levels (BG; either 10 or 12 log photons/cm^2/s; n = 9 RGCs). **D**: Average (± SEM) power spectral density (PSD) of the visually responsive RGCs under dark-adapted and two light-adapted conditions with background (BG) of either 10 or 12 log photons/cm^2/s (n = 9 RGCs). aCSF = artificial cerebrospinal fluid; MFA = meclofenamic acid. *** p=0.0006, **** p<0.0001.

(aCSF) conditions, the activity of these cells is directly influenced by the intrinsically oscillating membrane potential of AII ACs, introducing a level of background noise upon which their ectopic light response is presumably superimposed. The increase in the SNR and the ΔFR under the MFA conditions highlight the potential of this approach to optimize optogenetic sight restoration because the SNR is crucial to signal processing in the visual system [33,34]. In a wider sense, these data confirm the suitability of MFA for reducing spontaneous activity in the GCL while targeting other cell types of the inner retina for opsin expression, opening the door to other types of optogenetic interventions for sight rehabilitation.

Meclofenamate sodium is a U.S. Food and Drug Administration (FDA)-approved routinely prescribed non-steroidal anti-inflammatory drug containing 50 to 100 mg of MFA. Oral administration for appropriate dosing in the retina may lead to complications [35] while topical ophthalmic administration might be a potential strategy [36]. Chronic intraretinal administration of MFA may be achieved with thermoresponsive hydrogels [37,38], through intravitreal

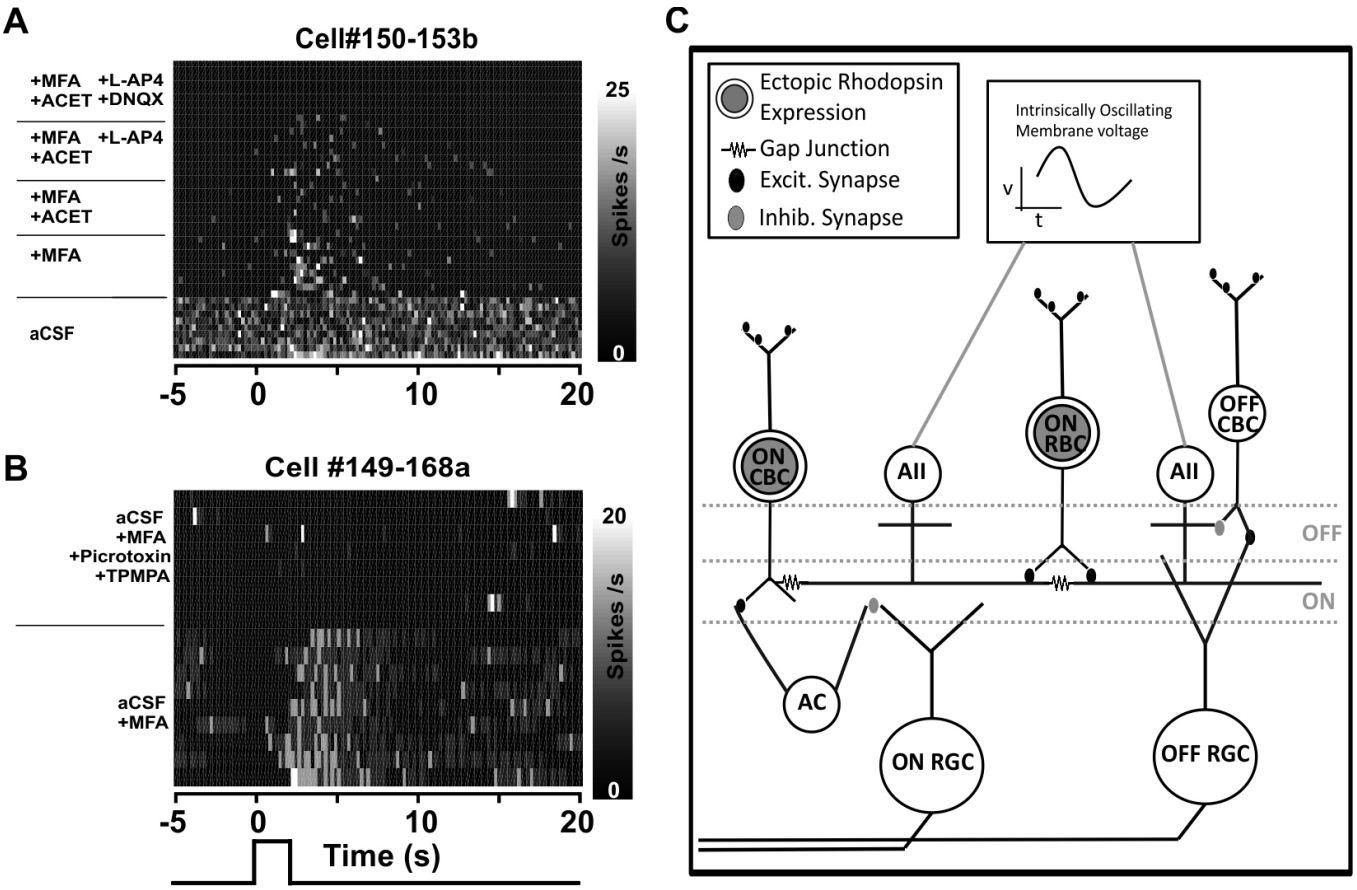

Figure 4. Pharmacological dissection of retinal circuits conveying signals from photosensitized bipolar cells. **A**: Example trial bin count (TBC) of light-responsive cell exposed to a 2 s light pulse (irradiance 10^{13} photons/cm^2/s) starting at time 0 s, with the progressive addition of drugs blocking glutamatergic signaling (trial order runs from bottom to top, with timing of the addition for individual agents indicated by the horizontal lines to left; note that once added the agent was included until the end of the trial, such that for this example the recording ended with artificial cerebrospinal fluid (aCSF), meclofenamic acid (MFA), ((S)-1-(2-amino-2-carboxyethyl)-3-(2-carboxy-5-phenylthiophene-3-yl-methyl)-5-methylpyrimidine-2,4-dione (ACET), L-AP4, and 6,7-dinitroquinoxaline-2,3-dione (DNQX) all included in the recording media. **B**: Example TBC of light-responsive cell exposed to a 2 s light pulse (irradiance 10^{13} photons/cm^2/s) at starting at time 0 s under the progressive addition of agents affecting the gamma-aminobutyric acid (GABA)ergic blockade (protocol and depiction as in **A**). **C**: A model of inner retinal circuitry following ectopic expression of rhodopsin in ON bipolar cells consistent with the pharmacological manipulations reported here. MFA blocks gap junctions, inhibiting propagation of oscillations originating in AII amacrine cells (ACs). MFA is also expected to block the transfer of signals from ON rod bipolar cells to ON cone bipolar cells via AII ACs but not transfer from ON rod bipolar cells to OFF cone bipolar cells or more direct signaling from ON cone bipolar cells. Inclusion of an inhibitory AC between the ON cone bipolar cell and the ON RGC allows for sign inversion to produce excitatory responses to light and accounts for the impact of the GABAergic blockade (**B**). CBCs= cone bipolar cells; RGCs = retinal ganglion cells; TPMPA = (1,2,5,6-tetrahydropyridin-4-yl)methylphosphinic acid.

[39] or suprachoroidal injections [40]. However, this drug affects all gap junctions, not just the AII cone–ON bipolar cell connection, and they are present between all classes of retinal neurons [41] and glia [42] making them heavily implicated in retinal coding [43,44], light adaptation [45,46], and cell survival [47]. Chronic retinal exposure to MFA may have adverse consequences in the long run. Conversely, a retina that lacks gap-junction coupling may prove to be a simpler, more stable environment, where engineering coherent light responses would be easier.

The widely used antimalarial drug mefloquine may prove to be an improvement on MFA as mefloquine has been shown to preferentially block CX36 gap junctions at nanomolar concentrations in N2A neuroblastoma cells [48] and in the rabbit retina at micromolar concentrations [49]. Although there are reports that the continuous use of mefloquine in patients results in secondary effects (such as anxiety, hallucinations, depression, psychoses, poor balance, and seizures [50,51]), these effects may not be experienced at the concentrations required to promote therapeutic effects in the retina.

RGCs receive input from RGCs, ACs, and bipolar cells, via gap junctions for RGCs and ACs [52,53], via all glutamate types for bipolar cells (for review, see [54]) and via GABA for ACs [55,56]. In the intact retina, rod-mediated vision relies in part on gap junction coupling, with the primary rod pathway relying on the AII AC to transmit ON signals through sign-conserving electrical synapses to ON cone bipolar cells (a parallel pathway via OFF cone bipolar cells employs a sign-inverting chemical synapse) [57,58]. However, there is mounting evidence that rod-mediated signals can reach the brain without gap-junction connectivity in the retina [59]. All the pharmacological experiments in the present study had an aCSF + MFA base; therefore, the only input to RGCs was from bipolar cells via glutamate neurotransmission and from ACs via GABAergic neurotransmission. Rod opsin is expected to have a hyperpolarization effect on the membrane voltage [60] of ON bipolar cells, where they are expressed because of the grm6 promoter in the virus. The fact that most of the responses observed here were excitatory suggests a disinhibition of RGC firing, with hyperpolarized bipolar cells acting upon inhibitory ACs targeting RGCs. This result fits with data from our previous study [5] and is corroborated by the fact that all responses disappeared under DNQX (AMPA-glutamate) blockade. We did not see an overall reduction in the number of responses following the application of MFA as would have been expected had the signal originated primarily in ON rod bipolar cells and reached RGCs via AII ACs and ON cone bipolar cells. One potential explanation for this finding is that the responses originated primarily with rod opsin expressed in the ON cone bipolar cells. Figure 4C presents a model illustrating this potential route of information transfer that is consistent with the ability of ionotropic glutamate and GABAergic inhibitors to block restored light responses. More complex routes employing OFF cone bipolar cells are also conceivable, as is the possibility that reorganization in the degenerate retina allows information generated in ON rod bipolar cells also to reach RGCs without relying on gap-junction connections.

Conclusions: This study supports the view that the non-steroidal anti-inflammatory and non-selective gap junction blocker MFA may have a role in improving the quality of vision provided by optogenetic therapies by reducing spontaneous activity and thus improving the SNR of the restored responses to light.

ACKNOWLEDGMENTS

We thank Jonathan Wynn for technical assistance and Annette Allen for helpful discussions. We also thank Stephanie Quinn for technical assistance in immunohistochemistry. This study was supported by grants from the ERC (268,970) and MRC (MR/N012992/1). Conflict of interest: The use of human rod opsin to restore visual function in advanced retinal degeneration is subject to a patent application currently licensed to Accucela Inc. for clinical development on which RJL and JCK are named inventors. The use of MFA in conjunction with rod opsin is not included in that patent nor the subject of any commercial development.

REFERENCES

1. Dowling JE, Sidman RL. Inherited retinal dystrophy in the rat. J Cell Biol 1962; 14:73-109. [PMID: 13887627].
2. Chang GQ, Hao Y, Wong F. Apoptosis: final common pathway of photoreceptor death in rd, rds, and rhodopsin mutant mice. Neuron 1993; 11:595-605. [PMID: 8398150].
3. Ahuja AK, Dorn JD, Caspi A, McMahon MJ, Dagnelie G, Dacruz L, Stanga P, Humayun MS, Greenberg RJ. Blind subjects implanted with the Argus II retinal prosthesis are able to improve performance in a spatial-motor task. Br J Ophthalmol 2011; 95:539-43. [PMID: 20881025].
4. Kitiratschky VBD, Stingl K, Wilhelm B, Peters T, Besch D, Sachs H, Gekeler F, Bartz-Schmidt KU, Zrenner E. Safety evaluation of "retina implant alpha IMS"aEuro"a prospective clinical trial. Graef Arch Clin Exp 2015; 253:381-7. [PMID: 25219982].
5. Cehajic-Kapetanovic J, Eleftheriou C, Allen AE, Milosavljevic N, Pienaar A, Bedford R, Davis KE, Bishop PN, Lucas RJ. Restoration of Vision with Ectopic Expression of Human Rod Opsin. Curr Biol 2015; 25:2111-22. [PMID: 26234216].

6. Bi A, Cui J, Ma YP, Olshevskaya E, Pu M, Dizhoor AM, Pan ZH. Ectopic expression of a microbial-type rhodopsin restores visual responses in mice with photoreceptor degeneration. Neuron 2006; 50:23-33. [PMID: 16600853].
7. Lin B, Koizumi A, Tanaka N, Panda S, Masland RH. Restoration of visual function in retinal degeneration mice by ectopic expression of melanopsin. Proc Natl Acad Sci USA 2008; 105:16009-14. [PMID: 18836071].
8. Van Gelder RN. Photochemical approaches to vision restoration. Vision Res 2015; 111:134-41. [PMID: 25680758].
9. Polosukhina A, Litt J, Tochitsky I, Nemargut J, Sychev Y, De Kouchkovsky I, Huang T, Borges K, Trauner D, Van Gelder RN, Kramer RH. Photochemical restoration of visual responses in blind mice. Neuron 2012; 75:271-82. [PMID: 22841312].
10. Tochitsky I, Polosukhina A, Degtyar VE, Gallerani N, Smith CM, Friedman A, Van Gelder RN, Trauner D, Kaufer D, Kramer RH. Restoring Visual Function to Blind Mice with a Photoswitch that Exploits Electrophysiological Remodeling of Retinal Ganglion Cells. Neuron 2014; 81:800-13. [PMID: 24559673].
11. Gaub BM, Berry MH, Holt AE, Reiner A, Kienzler MA, Dolgova N, Nikonov S, Aguirre GD, Beltran WA, Flannery JG, Isacoff EY. Restoration of visual function by expression of a light-gated mammalian ion channel in retinal ganglion cells or ON-bipolar cells. Proc Natl Acad Sci USA 2014; 111:E5574-83. [PMID: 25489083].
12. Bareket L, Waiskopf N, Rand D, Lubin G, David-Pur M, Ben-Dov J, Roy S, Eleftheriou C, Sernagor E, Cheshnovsky O, Banin U, Hanein Y. Semiconductor nanorod-carbon nanotube biomimetic films for wire-free photostimulation of blind retinas. Nano Lett 2014; 14:6685-92. [PMID: 25350365].
13. Jones BW, Kondo M, Terasaki H, Lin Y, McCall M, Marc RE. Retinal remodeling. Jpn J Ophthalmol 2012; 56:289-306. [PMID: 22644448].
14. Marc RE, Jones BW, Anderson JR, Kinard K, Marshak DW, Wilson JH, Wensel T, Lucas RJ. Neural reprogramming in retinal degeneration. Invest Ophthalmol Vis Sci 2007; 48:3364-71. [PMID: 17591910].
15. Jones BW, Watt CB, Marc RE. Retinal remodelling. Clin Exp Optom 2005; 88:282-91. [PMID: 16255687].
16. Stasheff SF. Emergence of sustained spontaneous hyperactivity and temporary preservation of OFF responses in ganglion cells of the retinal degeneration (rd1) mouse. J Neurophysiol 2008; 99:1408-21. [PMID: 18216234].
17. Drager UC, Hubel DH. Studies of visual function and its decay in mice with hereditary retinal degeneration. J Comp Neurol 1978; 180:85-114. [PMID: 649791].
18. Margolis DJ, Newkirk G, Euler T, Detwiler PB. Functional stability of retinal ganglion cells after degeneration-induced changes in synaptic input. J Neurosci 2008; 28:6526-36. [PMID: 18562624].
19. Menzler J, Zeck G. Network oscillations in rod-degenerated mouse retinas. J Neurosci 2011; 31:2280-91. [PMID: 21307264].
20. Biswas S, Haselier C, Mataruga A, Thumann G, Walter P, Muller F. Pharmacological analysis of intrinsic neuronal oscillations in rd10 retina. PLoS One 2014; 9:e99075-[PMID: 24918437].
21. Margolis DJ, Gartland AJ, Singer JH, Detwiler PB. Network oscillations drive correlated spiking of ON and OFF ganglion cells in the rd1 mouse model of retinal degeneration. PLoS One 2014; 9:e86253-[PMID: 24489706].
22. Borowska J, Trenholm S, Awatramani GB. An intrinsic neural oscillator in the degenerating mouse retina. J Neurosci 2011; 31:5000-12. [PMID: 21451038].
23. Trenholm S, Borowska J, Zhang JW, Hoggarth A, Johnson K, Barnes S, Lewis TJ, Awatramani GB. Intrinsic oscillatory activity arising within the electrically coupled AII amacrine-ON cone bipolar cell network is driven by voltage-gated Na plus channels. J Physiol 2012; 590:2501-17. [PMID: 22393249].
24. Toychiev AH, Ivanova E, Yee CW, Sagdullaev BT. Block of gap junctions eliminates aberrant activity and restores light responses during retinal degeneration. J Neurosci 2013; 33:13972-7. [PMID: 23986234].
25. Barrett JM, Degenaar P, Sernagor E. Blockade of pathological retinal ganglion cell hyperactivity improves optogenetically evoked light responses in rd1 mice. Front Cell Neurosci 2015; 9:330-[PMID: 26379501].
26. Barrett JM, Hilgen G, Sernagor E. Dampening Spontaneous Activity Improves the Light Sensitivity and Spatial Acuity of Optogenetic Retinal Prosthetic Responses. Sci Rep 2016; 6:33565-[PMID: 27650332].
27. Gaub BM, Berry MH, Holt AE, Isacoff EY, Flannery JG. Optogenetic Vision Restoration Using Rhodopsin for Enhanced Sensitivity. Mol Ther 2015; [PMID: 26137852].
28. Dhingra A, Sulaiman P, Xu Y, Fina ME, Veh RW, Vardi N. Probing neurochemical structure and function of retinal ON bipolar cells with a transgenic mouse. J Comp Neurol 2008; 510:484-96. [PMID: 18671302].
29. Vardi N, Morigiwa K. ON cone bipolar cells in rat express the metabotropic receptor mGluR6. Vis Neurosci 1997; 14:789-94. [PMID: 9279006].
30. Kim DS, Ross SE, Trimarchi JM, Aach J, Greenberg ME, Cepko CL. Identification of molecular markers of bipolar cells in the murine retina. J Comp Neurol 2008; 507:1795-810. [PMID: 18260140].
31. Haverkamp S, Wassle H. Immunocytochemical analysis of the mouse retina. J Comp Neurol 2000; 424:1-23. [PMID: 10888735].
32. Goo YS, Ye JH, Lee S, Nam Y, Ryu SB, Kim KH. Retinal ganglion cell responses to voltage and current stimulation in wild-type and rd1 mouse retinas. J Neural Eng 2011; 8:035003-[PMID: 21593549].

33. Vidne M, Ahmadian Y, Shlens J, Pillow JW, Kulkarni J, Litke AM, Chichilnisky EJ, Simoncelli E, Paninski L. Modeling the impact of common noise inputs on the network activity of retinal ganglion cells. J Comput Neurosci 2012; 33:97-121. [PMID: 22203465].

34. Dunn FA, Rieke F. The impact of photoreceptor noise on retinal gain controls. Curr Opin Neurobiol 2006; 16:363-70. [PMID: 16837189].

35. Fries JF, Williams CA, Bloch DA. The relative toxicity of nonsteroidal antiinflammatory drugs. Arthritis Rheum 1991; 34:1353-60. [PMID: 1953813].

36. Ahuja M, Dhake AS, Sharma SK, Majumdar DK. Topical ocular delivery of NSAIDs. AAPS J 2008; 10:229-41. [PMID: 18437583].

37. Misra GP, Singh RS, Aleman TS, Jacobson SG, Gardner TW, Lowe TL. Subconjunctivally implantable hydrogels with degradable and thermoresponsive properties for sustained release of insulin to the retina. Biomaterials 2009; 30:6541-7. [PMID: 19709741].

38. Park D, Shah V, Rauck BM, Friberg TR, Wang YD. An Anti-angiogenic Reverse Thermal Gel as a Drug-Delivery System for Age-Related Wet Macular Degeneration. Macromol Biosci 2013; 13:464-9. [PMID: 23316011].

39. Choonara YE, Pillay V, Danckwerts MP, Carmichael TR, du Toit LC. A review of implantable intravitreal drug delivery technologies for the treatment of posterior segment eye diseases. J Pharm Sci 2010; 99:2219-39. [PMID: 19894268].

40. Moisseiev E, Loewenstein A, Yiu G. The suprachoroidal space: from potential space to a space with potential. Clin Ophthalmol 2016; 10:173-8. [PMID: 26869750].

41. Bloomfield SA, Volgyi B. The diverse functional roles and regulation of neuronal gap junctions in the retina. Nat Rev Neurosci 2009; 10:495-506. [PMID: 19491906].

42. Zahs KR, Newman EA. Asymmetric gap junctional coupling between glial cells in the rat retina. Glia 1997; 20:10-22. [PMID: 9145301].

43. Grimes WN, Schwartz GW, Rieke F. The synaptic and circuit mechanisms underlying a change in spatial encoding in the retina. Neuron 2014; 82:460-73. [PMID: 24742466].

44. Schnitzer MJ, Meister M. Multineuronal firing patterns in the signal from eye to brain. Neuron 2003; 37:499-511. [PMID: 12575956].

45. Janssen-Bienhoid U, Trumpler J, Hilgen G, Schultz K, Muller LPD, Sonntag S, Dedek K, Dirks P, Willecke K, Weiler R. Connexin57 Is Expressed in Dendro-dendritic and Axo-axonal Gap Junctions of Mouse Horizontal Cells and Its Distribution Is Modulated by Light. J Comp Neurol 2009; 513:363-74. [PMID: 19177557].

46. Dedek K, Pandarinath C, Alam NM, Wellershaus K, Schubert T, Willecke K, Prusky GT, Weiler R, Nirenberg S. Ganglion cell adaptability: does the coupling of horizontal cells play a role? PLoS One 2008; 3:e1714-[PMID: 18320035].

47. Akopian A, Atlasz T, Pan F, Wong S, Zhang Y, Volgyi B, Paul DL, Bloomfield SA. Gap Junction-Mediated Death of Retinal Neurons Is Connexin and Insult Specific: A Potential Target for Neuroprotection. J Neurosci 2014; 34:10582-91. [PMID: 25100592].

48. Cruikshank SJ, Hopperstad M, Younger M, Connors BW, Spray DC, Srinivas M. Potent block of Cx36 and Cx50 gap junction channels by mefloquine. Proc Natl Acad Sci USA 2004; 101:12364-9. [PMID: 15297615].

49. Pan F, Mills SL, Massey SC. Screening of gap junction antagonists on dye coupling in the rabbit retina. Vis Neurosci 2007; 24:609-18. [PMID: 17711600].

50. Weinke T, Trautmann M, Held T, Weber G, Eichenlaub D, Fleischer K, Kern W, Pohle HD. Neuropsychiatric side effects after the use of mefloquine. Am J Trop Med Hyg 1991; 45:86-91. [PMID: 1867351].

51. Hennequin C, Bouree P, Bazin N, Bisaro F, Feline A. Severe psychiatric side effects observed during prophylaxis and treatment with mefloquine. Arch Intern Med 1994; 154:2360-2. [PMID: 7944858].

52. Volgyi B, Pan F, Paul DL, Wang JT, Huberman AD, Bloomfield SA. Gap junctions are essential for generating the correlated spike activity of neighboring retinal ganglion cells. PLoS One 2013; 8:e69426-[PMID: 23936012].

53. Brivanlou IH, Warland DK, Meister M. Mechanisms of concerted firing among retinal ganglion cells. Neuron 1998; 20:527-39. [PMID: 9539126].

54. Yang XL. Characterization of receptors for glutamate and GABA in retinal neurons. Prog Neurobiol 2004; 73:127-50. [PMID: 15201037].

55. Greferath U, Grunert U, Muller F, Wassle H. Localization of GABAA receptors in the rabbit retina. Cell Tissue Res 1994; 276:295-307. [PMID: 8020065].

56. Wassle H, Koulen P, Brandstatter JH, Fletcher EL, Becker CM. Glycine and GABA receptors in the mammalian retina. Vision Res 1998; 38:1411-30. [PMID: 9667008].

57. Deans MR, Volgyi B, Goodenough DA, Bloomfield SA, Paul DL. Connexin36 is essential for transmission of rod-mediated visual signals in the mammalian retina. Neuron 2002; 36:703-12. [PMID: 12441058].

58. Volgyi B, Deans MR, Paul DL, Bloomfield SA. Convergence and segregation of the multiple rod pathways in mammalian retina. J Neurosci 2004; 24:11182-92. [PMID: 15590935].

59. Brown TM, Allen AE, Wynne J, Paul DL, Piggins HD, Lucas RJ. Visual responses in the lateral geniculate evoked by Cx36-independent rod pathways. Vision Res 2011; 51:280-7. [PMID: 20709095].

60. Scott K, Becker A, Sun YM, Hardy R, Zuker CG. (Q-Alpha) Protein Function in-Vivo - Genetic Dissection of Its Role in Photoreceptor Cell Physiology. Neuron 1995; 15:919-27. [PMID: 7576640].

Articles are provided courtesy of Emory University and the Zhongshan Ophthalmic Center, Sun Yat-sen University, P.R. China. The print version of this article was created on 16 June 2017. This reflects all typographical corrections and errata to the article through that date. Details of any changes may be found in the online version of the article.